NASA TECHNICAL NOTE

NASA TN D-2132

NASA TN D-2132

ON THE EQUILIBRIUM SONIC-FLOW METHOD FOR EVALUATING ELECTRIC-ARC AIR-HEATER PERFORMANCE

by Warren Winovich

Ames Research Center
Moffett Field, California

NATIONAL AERONAUTICS AND SPACE ADMINISTRATION • WASHINGTON, D. C. • MARCH 1964

ON THE EQUILIBRIUM SONIC-FLOW METHOD FOR EVALUATING ELECTRIC-ARC AIR-HEATER PERFORMANCE

By Warren Winovich

Ames Research Center
Moffett Field, Calif.

NATIONAL AERONAUTICS AND SPACE ADMINISTRATION

For sale by the Office of Technical Services, Department of Commerce,
Washington, D.C. 20230 -- Price $1.00

ON THE EQUILIBRIUM SONIC-FLOW METHOD FOR EVALUATING ELECTRIC-ARC AIR-HEATER PERFORMANCE

By Warren Winovich

SUMMARY

The assumption that the air flow up to the sonic point in the discharge nozzle of an air heater can be represented by an isentropic expansion under equilibrium conditions is used to show that the flow rate and the heater reservoir pressure uniquely relate the total enthalpy level of the air. The relation is described by an empirical equation in closed form for pressures from 0.1 to 100 atmospheres and enthalpy levels up to 10,000 Btu/lb. A discussion of the method, the assumptions, and the applications to electric-arc air heaters is presented. Comparisons of the enthalpy measured by the present method and by heat-transfer measurement show good agreement.

INTRODUCTION

The measurement of the total enthalpy of air flows is of fundamental importance for high-temperature flow devices. For example, it is a governing factor in establishing the specific properties of the air stream. Similarly, for electric-arc propulsion devices the efficiency and thrust are related to the total enthalpy of the efflux. Moreover, in order to compare quantitatively the results obtained from very high-temperature, air-flow devices, it is essential to determine the total enthalpy. This report is concerned with a method for establishing the total enthalpy of air flows from high-temperature air heaters - principally electric-arc heaters operating in the real-gas region where dissociation effects are pronounced. Although the arc air-heater is emphasized, the method and techniques are generally applicable to other gases (such as CO_2, H_2, N_2, A) and other heater designs (e.g., resistance heater, pebble bed heater, etc.).

Since about 1957, there has been a widespread adoption and development of the electric-arc air heater. A variety of designs has appeared (e.g., refs. 1-6). Generally, the methods employed for determining the total enthalpy have been almost as varied as the designs. For example, in reference 2, enthalpy was determined from a measurement of stagnation heating rate; whereas, in reference 5, an energy balance method was employed. Others have employed emission spectroscopy methods (e.g., ref. 7) to determine the enthalpy level. The method examined here is based on the relation between the enthalpy of air in a reservoir, and the rate of flow of that air at equilibrium isentropic conditions through a choked nozzle; the method will hereinafter be referred to as the sonic-flow method.

Although the basic principle of the sonic-flow method has been employed by others (e.g., ref. 8), in the present report the sonic-flow-enthalpy relation is derived in closed mathematical form. The solution presented is approximate; however, the uncertainty involved is considered satisfactory for arc-heater

applications. The method as presented here is advantageous in that only simple state measurements are required. Moreover, the closed form allows the derivation of scaling laws for assessing the importance of the variables that determine heater performance. The report also includes a discussion of the effects of non-equilibrium air conditions, heat transfer, and boundary-layer flow on the sonic-flow method.

SYMBOLS

A	surface area of nozzle, ft^2
A^*	throat area of sonic nozzle, ft^2
c_p	specific heat, Btu/lb ^oR
C_D	discharge coefficient of nozzle
d^*	throat diameter of sonic nozzle, ft
f	mass fraction of atomic oxygen, particles O per atom of air/0.21
g_c	conversion factor, 32.2 lb ft/lb_f sec^2
h	enthalpy, Btu/lb
H	heat-transfer coefficient, Btu/sec ft^2 ^oR
J	conversion factor, 778 ft-lb_f/Btu
k	reaction rate constant, $cm^2/mole^2 sec$
K_c	equilibrium constant for reaction rates
l	characteristic length in Reynolds number
m	molecular weight, lb/mole
n	exponent in boundary-layer profile equation, $\frac{u}{V_\infty} = \left(\frac{y}{\delta}\right)^{1/n}$
Nu	Nusselt number
Pr	Prandtl number
p	pressure, atm
p_a	standard atmosphere, 2,115 lb_f/ft^2 atm
$\dot{q}$	heating rate, Btu/sec ft^2
Q	total heat transfer, Btu/sec

r	nozzle radius, ft
r_i	inlet radius of nozzle, ft
r^*	throat radius of sonic nozzle, ft
R	universal gas constant, 1,545 ft-lb_f/mole ^oR
Re	Reynolds number
S	entropy, Btu/lb ^oR
T	absolute temperature, ^oR
u	local velocity, ft/sec
V	free-stream velocity, ft/sec
w	mass flow rate, lb/sec
W	shear energy, Btu/lb
y	distance measured from nozzle wall, ft
z	molecular weight ratio for dissociated air, $\frac{m_a}{m}$
γ	ratio of specific heats
δ	boundary-layer thickness, ft
ρ	density, lb/ft^3
μ	absolute viscosity, lb/sec ft
τ	time, sec

Subscripts and Superscripts

2	state behind normal shock
a	standard atmosphere
s	constant entropy
t	stagnation state
w	wall value
z	constant molecular weight ratio

*	sonic value
∞	free-stream value
$(\bar{})$	mean value
adiabatic	flow with no heat transfer
diabatic	flow with heat transfer
vib	vibrational relaxation
rec	recombination

EQUILIBRIUM SONIC-FLOW METHOD

An expression for the total enthalpy level of the air flow produced by an arc heater can be derived in terms of the arc-heater operating conditions. It is shown below that the flow rate through a sonic nozzle is uniquely determined by the operating pressure and total enthalpy in the arc-heater reservoir. Conversely, if the air flow is metered and the pressure is measured, the total enthalpy is defined for an arc-heater effluent discharging at sonic speed through a nozzle. The expression is readily derived for air as a perfect gas, and can be extended to both a calorically imperfect gas (variable specific heat), and a calorically and thermally imperfect gas (i.e., a real gas; variable specific heat and dissociation). Results similar to the analysis given here are available for low-temperature air flows in general form. However, the details are reviewed here to emphasize the various flow regions and to establish a reference background for later discussions of the method.

The process to be considered is described by the following sketch and assumptions:

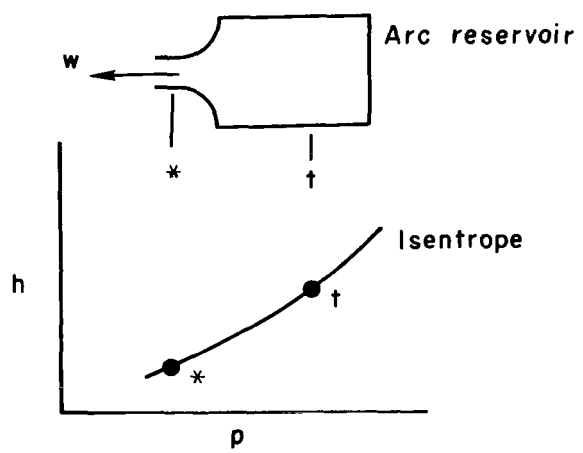

The assumptions one must make to derive the relation are listed below:

1. The flow is in thermal equilibrium.

2. The flow is isentropic.

3. The flow is one-dimensional and homogeneous.

4. The flow is steady with time.

(In a later discussion, the effects of some of the important departures from this idealized model will be examined.)

The equations governing the flow through the nozzle of an arc heater are as follows:

Continuity	$w = \rho VA$	(1)
Energy	$h_t = h + V^2/2g_cJ$	(2)
State	$\rho = pp_a(R/m)T$	(3)
Process	$dp/p = \gamma d\rho/\rho$ (ds = 0, isentropic flow)	(4)

With sonic velocity at the nozzle throat, the mass velocity is

$$w/A^* = \rho^* V^* \tag{5}$$

This can be represented in terms of reservoir conditions by use of equations (1) to (3). The resulting equation applicable to either a perfect or real gas flow is

$$\frac{w}{A^* p_t} = \frac{p_a\sqrt{g_cJ}}{R/m}\frac{\sqrt{h_t}}{T_t}\left\{\frac{\rho^*}{\rho_t}\left[2\left(1 - \frac{h^*}{h_t}\right)\right]^{1/2}\right\} \tag{6}$$

Expression for Enthalpy for Various Gas Conditions

Perfect gas.- When air behaves as a perfect gas, the sonic-flow relation given by equation (6) reduces to the simpler form (ref. 9)

$$\frac{w}{A^* p_t} = \frac{p_a\sqrt{g_c/J}}{\sqrt{h_t}}\sqrt{\frac{\gamma 2}{\gamma - 1}\left(\frac{2}{\gamma + 1}\right)^{\frac{\gamma+1}{\gamma-1}}} \tag{7}$$

For low-temperature air with $\gamma = 7/5$, the last term has the value 1.281 and when the other constants in equation (7) are substituted, the result for air as a perfect gas is

$$\frac{w}{A^* p_t} = \frac{551}{\sqrt{h_t}} \tag{8}$$

where $h_t < 250$ Btu/lb which is the region wherein air is approximated by a perfect gas with $\gamma = 7/5$.

Calorically imperfect gas.- When air behaves as a calorically imperfect gas, the specific heat ratio is dependent on the temperature. However, since no dissociation of molecules occurs, the equation of state remains the same as for a perfect gas. This condition is closely approximated for air over the enthalpy range from 250 to about 1,000 Btu/lb for pressures above 1/10 atmosphere. Arc-type air heaters generally operate above 1/10 atmosphere. This defines the region of the high-pressure arc (ref. 10). For this range, enthalpy can be expressed as

$$h = \int_o^T c_p \, dT = \frac{R/m}{J} \int_o^T \frac{\gamma}{\gamma - 1} \, dT \tag{9}$$

where γ is a function of temperature only. From equations (4), (6), and (9), the sonic-flow relation for a calorically imperfect gas is

$$\frac{w}{A^* p_t} = \frac{p_a \sqrt{\frac{g_c}{J}}}{\sqrt{h_t}} \left\{ \left(\frac{1}{T_t} \int_o^{T_t} \frac{\gamma}{\gamma - 1} \, dT \right) \sqrt{2 \left(1 - \frac{\int_o^{T^*} \frac{\gamma}{\gamma - 1} \, dT}{\int_o^{T_t} \frac{\gamma}{\gamma - 1} \, dT} \right)} \left[e^{-\int_{T^*}^{T_t} \left(\frac{1}{\gamma - 1} \right) \frac{1}{T} \, dT} \right] \right\} \tag{10}$$

The term in the braces has been evaluated numerically from the tables of reference 11 for temperatures up to 4,000° R (about 1,000 Btu/lb). An equation has been fitted to the result to obtain the sonic-flow relation in closed form

$$\frac{w}{A^* p_t} = \frac{551}{\sqrt{h_t}} \left[1 + 4.89 \times 10^{-5} (h_t - 250) \right] \tag{11}$$

where $250 \leq h_t \leq 1{,}000$ Btu/lb. This result shows only a small deviation from the perfect gas result up to the enthalpy level of 1,000 Btu/lb where oxygen dissociation becomes significant.

Real gas.- For air at enthalpy levels greater than 1,000 Btu/lb, the dissociation of oxygen becomes significant. Because of dissociation, both the molecular weight of the mixture and the specific heat ratio become dependent on pressure as well as on temperature. Consequently, no simple formulation of specific heat ratio or molecular weight ratio can be written similar to equation (9).

Moreover, additional equations relating the dissociation phenomenon to the state of the gas are required to solve the sonic-flow relation. In view of these complications that arise for air at elevated temperatures, the method for obtaining the sonic-flow relation presented here is derived from an empirical analysis.

The method used is based on the procedure given in reference 12 for obtaining the mass velocity at the sonic point (i.e., $\rho^*V^* \equiv w/A^*$); the procedure is a trial-and-error calculation in which equations (1) to (4) and the equation of state from reference 9 are used. The calculations were made for several pressures for enthalpies between 1,000 and 10,000 Btu/lb. The pressure range covered the interval from 1/4 to 100 atmospheres. Results of the calculations show that for all pressures, the value w/A^*p_t falls within 4 percent of a mean curve. The equation of this curve was taken as the solution for the sonic-flow expression for air which is both calorically and thermally imperfect. The least squares fit to the calculations is

$$\frac{w}{A^*p_t} = \frac{280}{h_t^{0.397}} \tag{12}$$

where $1{,}000 < h_t < 10{,}000$ Btu/lb. At an enthalpy level of 1,035 Btu/lb, this solution matches that for calorically imperfect air.

The sonic-flow relations for the three cases considered are shown in graphical form in figure 1. The dashed lines at 250 and 1,000 Btu/lb denote the upper limits of application of the perfect-gas relation (eq. (8)) and the calorically imperfect gas relation (eq. (11)), respectively. Above 1,000 Btu/lb, the curve represented by equation (12) formulates the sonic-flow relation adequately for most purposes. The over-all formulation yields the total enthalpy level of the stream in terms of rather easily measured quantities: the flow rate, the nozzle size, and the reservoir pressure. The small pressure dependency in the real-gas region can be reduced by a special testing technique applied in conjunction with the sonic-flow formulation as described in the next section.

Enthalpy determination by pressure-rise technique.- The technique of operating an arc heater while the flow rate is constant before and after the arc is initiated is an important application of the sonic-flow method. To establish constant flow, the pressure of the air supply is greater than twice the reservoir pressure when the arc is on, and the flow is controlled with a throttling valve ahead of the heater. When constant flow is established, the equlibrium sonic-flow relation is used to determine the total enthalpy in the heater reservoir from the observed pressure rise following the initiation of the arc. The determination is made in the following manner: First, one can write

$$\frac{(p_t)_{run}}{(p_t)_{start}} = \frac{\left(\frac{w}{A^*p_t}\right)_{start}}{\left(\frac{w}{A^*p_t}\right)_{run}} = \frac{\frac{551}{\sqrt{(h_t)_{start}}}}{\left(\frac{w}{A^*p_t}\right)_{run}} \tag{13}$$

where the sonic-flow relation (w/A^*p_t) is taken from either equation (8), (11), or (12), depending on the enthalpy level. With air entering the unit at 72° F, for example, the cold flow (starting) enthalpy is 128 Btu/lb, the pressure-rise relation is

$$\frac{(p_t)_{run}}{(p_t)_{start}} = \frac{48.7}{\left(\frac{w}{A^*p_t}\right)_{run}} \tag{14}$$

Figure 2 shows the total enthalpy in terms of the pressure-rise ratio. In the curves of figure 2 for the real-gas region, individual calculated point values were used rather than values from equation (12). In this way, the small pressure dependency noted earlier can be taken into account by interpolating between the curves of figure 2.

DISCUSSION

The expected departures of actual nozzle flow conditions from the idealized flow conditions will be evaluated. The assessment will consider the effects of (1) nonequilibrium air conditions, (2) nozzle wall heat transfer, and (3) boundary-layer flow. The objectives will be to define the range of applicability and the corrections necessary for the idealized equilibrium, isentropic, one-dimensional nozzle flows.

Finally, the application of the pressure-rise technique for determining total enthalpy will be discussed. Some experimental results obtained with the rotating-arc air heater described in references 6 and 13 provide a comparison of the enthalpy values given by sonic flow with corresponding values found by measurements of stagnation-point heating rates on hemispheres.

Nonequilibrium Flow Effects

The assumption of thermodynamic equilibrium is explicit in the formulation of the sonic-flow relation. In typical circular-arc nozzle inlets the time required for the air to flow up to the sonic throat is short - of the order 100 microseconds. The question arises, then, whether there is sufficient time for all species to attain the equilibrium state. The associated question is, if the time is not sufficient, what error will be introduced into the sonic-flow relation by the occurrence of nonequilibrium flow. The discussion of these two questions will cover the enthalpy range between 1,000 and 10,000 Btu/lb, and the pressure range between 0.1 to 100 atmospheres.

Vibrational relaxation.- At the elevated air temperatures encountered in arc heaters, the vibrational energy modes for the diatomic molecules are active. The shock-tube measurements of reference 14 give vibrational relaxation times for the enthalpy range considered here. These relaxation times are compared in figure 3

with flow transit times for a family of circular-arc inlets with inlet radii between 1/2 and 2 inches. This range is representative of the principal dimensions found for the nozzles of present arc heaters. Although specific geometry differs, most inlets are no longer than a few inches. Thus, the transit times can be represented by the band shown on figure 3. Typically, the transit times are found to be 10^{-5} to 10^{-4} seconds in duration. For the high-pressure arc ($p > 0.1$ atm), the vibrational relaxation times are very much smaller. Consequently, it appears that the flow will be in vibrational equilibrium for all conditions in which the nozzle inlet is over an inch in length.

Chemical relaxation.- The situation with regard to chemical relaxation has been analyzed for the air model represented by the reaction

$$4N_2 + O_2 \leftrightarrows 4N_2 + (1-f)O_2 + 2fO \tag{15}$$

where f, the mass fraction of atomic oxygen present, depends upon the degree of dissociation of the oxygen molecules. (Note that this model approximates air between enthalpy levels of 1,000 and 10,000 Btu/lb.) Values of f are obtained from the equilibrium calculations of reference 11. As enthalpy increases from 1,000 Btu/lb, f increases from zero (no dissociation) to unity, corresponding to complete dissociation of oxygen at about 8,000 Btu/lb, depending slightly on the pressure level.

The dissociation rates for oxygen given in reference 14 have been applied to the chemical model used here to determine whether there is sufficient time for the reverse reaction (i.e., recombination) to occur. The recombination rates used here have been deduced from the dissociation rate measurements by applying the equilibrium constant to obtain

$$k_r = k_f/K_c$$

The validity of this equilibrium relation as applied to the transient recombination phenomenon has been experimentally verified in reference 15. For the chemical reaction assumed, the chemical recombination time is given by the relation

$$\tau_{rec} = \frac{1}{2k_r[O]_{\tau=0}[N_2]} \tag{16}$$

where the terms in the brackets are the molecular concentrations of atomic oxygen and nitrogen. For the calculation, it was assumed that the concentration of nitrogen was constant, and the values for the concentration of atomic oxygen were computed from reference 11.

As indicated by equation (16), the chemical recombination time varies inversely as the product of the particle densities. Since the particle densities are proportional to the pressure, the recombination time varies inversely as the square of the pressure which is characteristic of the three-body collision

process. For the high-pressure arc range, the recombination times computed from equation (16) are shown in figure 4. The nozzle transit time is again superposed on the same plot. For pressures below 10 atmospheres, the flow through typical nozzles will be chemically frozen since the transit time will be considerably shorter than the recombination time. For very high pressures (over 200 psi, say), the flow will be in complete thermodynamic equilibrium.

The results shown in figures 3 and 4 indicate that the air will be in vibrational equilibrium at all pressures but will expand in a chemically frozen mode for all pressures below about 10 atmospheres. Accordingly, the sonic-flow relation is affected by the chemically frozen flow. In the following section, the air model employed (eq. (15)) is used to determine the magnitude of the correction to the sonic-flow relation due to freezing of the chemical species at low pressures (below 10 atmospheres, typically).

For low-pressure nozzle flow, the flow rate for frozen chemical composition can be written in terms of the equilibrium value as

$$\frac{w_z}{w_s} = \frac{(\rho^* V^*)_z}{(\rho^* V^*)_s} = \left\{ \frac{\left(\frac{p^*}{p_t}\right)_z}{\left(\frac{p^*}{p_t}\right)_s} \sqrt{\frac{\gamma_z}{\gamma_s}} \sqrt{\frac{z_s^*}{z_z^*}} \right\} \sqrt{\frac{\left(\frac{T^*}{T_t}\right)_s}{\left(\frac{T^*}{T_t}\right)_z}} \tag{17}$$

One can readily verify that the term in the braces is within a fraction of a percent of unity for all high-pressure arc conditions by comparing the term in the braces to the exact relation (see ref. 9). Recognizing this, the sonic-flow-rate ratio simply becomes

$$\frac{w_z}{w_s} = \sqrt{\frac{\left(\frac{T^*}{T_t}\right)_s}{\left(\frac{T^*}{T_t}\right)_z}} \tag{18}$$

By comparing figures 3 and 4, it is seen that vibrational equilibrium will exist even when the flow is chemically frozen. This fact suggests that the ratio given by equation (18) can be evaluated if the frozen mixture is considered to expand isentropically as a perfect gas with the isentropic coefficient determined by the reservoir conditions. Then,

$$\frac{w_z}{w_s} = \sqrt{\frac{\gamma_z + 1}{\gamma_s + 1}} \tag{19}$$

The isentropic coefficients have been determined through the high-pressure arc range from the chemical equation of the air model (eq. (15)) and from the tabulated species concentrations given in reference 11. Results of these calculations are summarized in figure 5. The table given below has been prepared from the results to give the ratio of w_z/w_s over the ranges in question.

w_z/w_s			
h	p = 0.1 atm	p = 1 atm	p = 10 atm
1,000	1.000	1.000	1.000
2,000	1.035	1.028	1.025
4,000	1.030	1.027	1.023
6,000	1.052	1.045	1.040
8,000	1.055	1.050	1.043
10,000	1.055	1.052	1.045

This table shows that the ratio is small and only very slightly affected by pressure over the range where it is applicable. No loss in generality occurs, then, if the small pressure effect is ignored. The procedure adopted here is to use the values of the ratio for the one atmosphere case (as indicated in the following paragraph) to correct the values of stagnation enthalpy for the effect of chemically frozen flow.

A general correction for nozzle inlet flow with frozen species can be obtained by differentiating the equilibrium sonic-flow relation (eq. (12)), and applying the values of the ratio shown in the preceding table; that is,

$$\frac{dh}{h} = -\frac{2}{2}\frac{dw}{w} = \frac{2}{2}\left(\frac{w_z}{w_s} - 1\right) \tag{20}$$

For the high-pressure arc in the range from 0.1 to 10 atmospheres, the enthalpy deduced from the equilibrium equation must be increased. The percentage increase is tabulated below for 1 atmosphere since, as noted, the effect of pressure is negligible.

h	dh/h
1,000	0
2,000	.070
4,000	.068
6,000	.113
8,000	.125
10,000	.130

The correction for frozen species becomes appreciable above enthalpy levels of 5,000 Btu/lb. It should be recognized that the inherent uncertainties in the measurements involved place a practical accuracy limit of about 5 percent on enthalpy determined by the sonic-flow method. This calculation cannot be extrapolated to enthalpy levels above 10,000 Btu/lb since at this level nitrogen begins to dissociate appreciably.

Heat-Transfer and Boundary-Layer-Displacement Effects

The isentropic assumption for the model analyzed implies no heat transfer or friction. For real flows, however, heat transfer and friction do occur, and they tend to alter the ideal, one-dimensional, isentropic values of enthalpy and flow rate. The irreversible effects are due to the formation of the boundary layer which gives rise to temperature and velocity gradients near the wall. Thus, irreversibility and two-dimensional effects occur simultaneously. These two effects influence the flow differently. Irreversible effects, principally heat transfer, reduce the stagnation enthalpy. The two-dimensional effect caused by the boundary layer gives rise to a nozzle discharge coefficient that alters the flow rate but does not affect stagnation enthalpy. The discharge coefficient must be taken into account, however, when applying the sonic flow relations (eqs. (8), (11), and (12)). The two effects will be considered separately in more detail in the following sections.

Irreversibility.- The energy equation for a real flow includes terms that take into account the energy lost as a result of heat transfer and the shear energy dissipated at the wall. Thus, for a steady flow rate w,

$$h_t = c_p T + \frac{V^2}{2g_c J} + \frac{Q}{w} + W \tag{21}$$

For arc-jet flows, the heating rates in the nozzle are high; consequently, the energy loss due to fluid shear is much less than that due to heat transfer.[1] Also, as will be shown, the effect of heat transfer is small. Therefore, for practical purposes, the shear energy term can be neglected.

The energy equation represented by equation (21) allows one to write an expression for the enthalpy loss due to irreversibility in the throat

$$\frac{h_{t,s} - h_t}{h_{t,s}} \doteq \frac{Q}{wh_{t,s}} \tag{22}$$

The departure from the isentropic value is small if the right side of equation (22) is small. The quantity on the right has been estimated in appendix A and it has been found for all cases to be less than 10 percent for typical arc-jet operations. This result indicates that stagnation enthalpy is only slightly reduced

[1]For conditions of $T_w/T_\infty \approx 1/8$, typical for arc jets, Reynolds analogy applied to the nozzle inlet predicts $(W/Q)w \approx 1/10$.

by convective heat transfer in rapidly converging inlets - even though heating rates are high. Consequently, the real flow does not depart much from the isentropic flow assumed in the analysis.

Two-dimensional effects.- In the determination of the discharge coefficient for real flow through a nozzle, the effects of both friction and heat transfer must be considered. Frictional shear in the boundary layer reduces the mass-flow rate by decreasing the velocity near the wall. Heat transfer, on the other hand, increases the mass flow because local density near the wall is increased from the adiabatic wall value. The local density increases near the wall, for constant pressure across the boundary layer, because of the lower temperatures encountered near the wall for diabatic flow. Therefore, in the determination of the integrated mass flow rate through a nozzle, the frictional and heat-transfer effects tend to counteract each other. The net effect on the mass-flow rate is dependent on the relative magnitude of the heat-transfer rate with respect to the wall shear.

The discharge coefficient is defined as the ratio of the actual flow rate to the ideal, one-dimensional, isentropic flow rate.

$$C_D = \frac{w}{w_s} \tag{23}$$

The discharge coefficient can be derived in closed form. Details are given in appendix B. The expression is given in terms of boundary-layer thickness and shape, which is determined by the shear forces, and the heat-transfer rate, which is characterized by the ratio of wall to free-stream temperature

$$\left.\begin{aligned} C_D &= \left(1 - \frac{\delta}{r^*}\right)^2 + 2\left(\frac{\delta}{r^*}\right)\int_0^1 \frac{\left(\frac{y}{\delta}\right)^{1/n}\left[1 - \left(\frac{\delta}{r^*}\right)\left(\frac{y}{\delta}\right)\right] d\left(\frac{y}{\delta}\right)}{\frac{z}{z_\infty}\left[\frac{T_w}{T_\infty} + \left(1 - \frac{T_w}{T_\infty}\right)\left(\frac{y}{\delta}\right)^{1/n}\right]} \\ \text{where} \quad \frac{z}{z_\infty} &\approx 1 - 0.15\left\{1 - \left[\frac{T_w}{T_\infty} + \left(1 - \frac{T_w}{T_\infty}\right)\left(\frac{y}{\delta}\right)^{1/n}\right]^3\right\} \end{aligned}\right\} \tag{24}$$

The basis of this equation is the similarity between velocity and temperature distributions in the turbulent boundary layer. This assumption has been verified experimentally for incompressible flows (ref. 16), and the compressible theory given in reference 17 predicts this result for a Prandtl number of 0.72 and high heating rates ($T_w/T_\infty \approx 1/8$).

The discharge coefficient of equation (24) has been evaluated by numerical integration to examine the effects of boundary-layer shape and thickness. To examine the shape effect, the exponent in the equation for velocity profile $u/V_\infty = (y/\delta)^{1/n}$ was varied from 1/5 to 1/11. The calculations were carried out for $T_w/T_\infty = 1/8$, which is typical for arc-jet operations with transient heat-sink or water-cooled copper nozzles. The results are shown in figure 6. For the very high heating rates encountered, the discharge coefficient actually exceeds unity by a small amount. The discharge coefficient is found to be insensitive to boundary-layer shape, and boundary-layer thickness as well, for the high heating rate conditions encountered in practice.

On the basis of the flat-plate theory of reference 18, the boundary-layer thickness is estimated to be in the range

$$\frac{1}{4} < \frac{\delta}{r^*} < \frac{1}{2}$$

for typical arc-jet nozzles. For this range of boundary-layer thickness, the diabatic discharge coefficient is essentially unity (fig. 6). For the limiting case of infinite heat transfer and no dissociation, equation (24) predicts a discharge coefficient of exactly unity.

At lower heating rates (i.e., $T_w/T_\infty > 1/4$), the discharge coefficient is less than unity. Values of the discharge coefficient have been calculated (eq. (24)) for the low heating rate range (i.e., $1/4 < T_w/T_\infty < 1.2$), and the results are shown in figure 7. The values of the discharge coefficient shown therein are for a 1/7-power velocity profile and a boundary-layer thickness of $\delta/r^* = 1/5$. For $T_w/T_\infty = 1.18$, the solution corresponds to the adiabatic wall case for $\gamma = 1.4$ and a Prandtl number of 0.72. The discharge coefficient can be experimentally determined for a nozzle by running cold-flow tests and applying equation (8) in conjunction with the discharge coefficient definition (eq. (23)). This has been done for a circular-arc nozzle inlet ($r_i/d^* = 5$) of 1/4-inch diameter. The Reynolds number of the test was 2×10^6. The result compared with the predicted discharge coefficient in figure 7 shows good agreement. In situations where the arc produces a very strong vortex in the nozzle throat, however, the discharge coefficient may be drastically altered, and the vortex may be different with the arc on than with the arc off. Strong vortex flows may alter the mass flow significantly (ref. 19).

The calculated results summarized in figures 6 and 7 allow one to assess the effects of boundary layer and heat transfer upon the sonic-flow relations (eqs. (8), (11), and (12)). Figure 6 indicates that for the range typical of arc-jet nozzles, the diabatic discharge coefficient is essentially equal to unity. From practical considerations, one may take the discharge coefficient to be one in view of the inherent uncertainty in the measurements of pressure and flow rate required for the sonic-flow relations.

For the enthalpy determination from the pressure-rise technique (eq. (14)), it would first appear that one must apply a correction for the cold-flow discharge coefficient as shown by figure 7. The adiabatic discharge coefficient may

be obtained directly by measurement or from simple flat-plate theory. The corrected form of the pressure-rise equation for a given enthalpy level becomes:

$$\frac{(p_t)_{run}}{(p_t)_{start}} = \left[\frac{(p_t)_{run}}{(p_t)_{start}}\right]_s \times \left[\frac{(C_D)_{adiabatic}}{(C_D)_{diabatic}}\right] \tag{25}$$

As shown in figure 7, the diabatic discharge coefficient can be taken as one. Since the adiabatic coefficient is always less than one, the boundary-layer correction increases the enthalpy by an amount dependent on the heating rate (fig. 7). The pressure-rise equations with the adiabatic discharge coefficient correction applied have been recalculated and are shown in figure 8. The correction is small at moderate enthalpies. Above about 1,000 Btu/lb, however, the enthalpy correction approaches a constant value given approximately by $(5/2)h_t[1 - (C_D)_{adiabatic}]$ for the boundary-layer effect.

The correction for heat transfer to the nozzle is made by applying equation (A9) to determine the enthalpy decrement in the throat region. The Reynolds number of the nozzle will vary with the enthalpy according to the sonic-flow relation[2] (eq. (12)). Consequently, as the enthalpy increases, the enthalpy decrement increases to oppose the boundary-layer correction. The extent of these opposing trends is shown in figure 8.

As seen from figure 8, the correction for the heat-transfer effect nearly offsets the correction for the boundary-layer effect. In view of this result, which is typical, as well as the inherent uncertainties in the corrections themselves, and the usual errors in the measurement of pressure in an arc-heater reservoir, it appears unnecessary to apply corrections for the boundary-layer and heat-transfer effects. (As previously shown, the correction for frozen species flows should be made when applicable.)

---

[2]The Reynolds number is given by:

$$Re = \frac{\rho^* V^* d^*}{\mu_\infty} = \frac{280\ p_t d^*}{(h_t)^{0.397}\mu_\infty} \qquad \text{for} \quad h_t > 1{,}000 \text{ Btu/lb}$$

where the viscosity is given by the empirical equation

$$\mu_\infty = 128\times10^{-7}\left(\frac{T_\infty}{T_w}\right)^{0.63} \frac{\text{lb}}{\text{sec ft}}$$

Combining these

$$Re \approx 2.2\times10^7 \left[\frac{p_t d^* \left(\frac{T_w}{T_\infty}\right)^{0.63}}{h_t^{0.40}}\right]; \qquad h_t > 1{,}000 \text{ Btu/lb}$$

Example Application of the Pressure-Rise Technique

An illustration of the pressure-rise technique and a record of the arc chamber pressure versus time is shown in figure 9. Before the arc was started, the chamber pressure was at some low value determined by the flow rate and starting enthalpy level (eq. (8)). After the arc voltage was applied, a short transient occurred, and the pressure increased to a constant mean value determined by the running enthalpy level (eq. (14)). During this starting transient, the sonic-flow equations do not apply (in accord with assumption 4). The real nature of the transient is indicated by the changing slope of the calorimeter trace in figure 9. The new energy level was essentially constant as indicated by constant high pressure level until the arc was shut off. The measured pressure-rise ratio of 4.6:1 and figure 2 indicate a total enthalpy of 4,500 Btu/lb. These data were obtained from the Ames low-contamination arc unit described in reference 13.

The heat-transfer rate measured by a center-line calorimeter provides an independent method for enthalpy determination. For a series of arc-jet tests, the enthalpy has been deduced from the measured stagnation-point, heat-transfer rate and measured stagnation pressure. Measurements were made in a 2-5/8-inch-diameter supersonic stream of Mach number about 3. The model was a 3/4-inch hemisphere cylinder. (See ref. 13.) The laminar theories of references 20 and 21 were used to deduce enthalpy from the measurements using a Lewis number of 1.0. The values of enthalpy deduced from measured heating rates are compared in figure 10 with the values of enthalpy determined from the sonic-flow relation and the pressure-rise technique. For the sonic-flow determination, the discharge coefficient was taken as unity for hot flow (i.e., eq. (12)). For the pressure-rise technique, the experimentally determined cold flow discharge coefficient shown in figure 7 was used (i.e., eq. (25)). It is evident from figure 10 that both methods gave essentially the same result. In addition, the enthalpy levels are in good agreement with the enthalpy deduced from simultaneously measured stagnation-point heating rates. The data scatter by about 10 percent about the line of perfect agreement.

CONCLUDING REMARKS

It has been shown that the total enthalpy of the air flow from the reservoir of an arc-type heater through a sonic nozzle is uniquely determined by the reservoir pressure and the steady mass flow rate through the device. For these results to be applicable, the energy must be imparted to the air in an essentially stagnant region. This would rule out, for example, such devices where the arc occurs through the nozzle and adds significant energy in the inlet or supersonic portion of the nozzle. For an equilibrium, isentropic sonic air flow, the enthalpy formulation was derived for application in three ranges of total enthalpy:

1. Perfect gas; $h < 250$ Btu/lb

2. Calorically imperfect gas; $250 < h < 1{,}000$ Btu/lb

3. Real gas; $1{,}000 < h_t < 10{,}000$ Btu/lb

The assumption of equilibrium nozzle flow which underlies the formulation has been critically reviewed. On the basis of the transit time of the flows up to the throats of typical nozzles and vibrational and dissociative relaxation times, the flows will be in vibrational equilibrium for practical ranges of reservoir pressures, and in dissociative equilibrium for reservoir pressures above about 10 atmospheres. For the nozzle inlet flows which will be chemically frozen for pressures below 10 atmospheres, the total enthalpy deduced from equilibrium sonic-flow relations will be low by about 13 percent at 10,000 Btu/lb.

Consideration was also given to errors in the formulation arising from the effects of irreversibility, heat transfer, and boundary layer. Effects of irreversibility (i.e., principally a reduction in enthalpy due to nozzle inlet heating) are shown to be small for typical inlet designs even though local heating rates may be high. It is demonstrated that the heat-transfer and boundary-layer effects yield compensating corrections to the total enthalpy deduced from the relations for equilibrium sonic flow. This result was shown to be due to the nozzle discharge coefficient approaching unity for the small wall to free-stream temperature ratios that always occur in the nozzle inlets of arc heaters.

Values of total enthalpy, determined for one particular arc-type heater by use of the equilibrium sonic-flow method, were compared with corresponding values deduced from a combination of measurements of stagnation heating rates and pressure, and an appropriate heating-rate theory. The comparison indicated that when the underlying assumptions of the equilibrium sonic-flow method are not seriously violated the enthalpy values predicted agree with the independent evaluation of the enthalpy level.

Ames Research Center
National Aeronautics and Space Administration
Moffett Field, Calif., Oct. 28, 1963

APPENDIX A

HEAT TRANSFER IN THE NOZZLE INLET

As the hot gases flow through the inlet region of a nozzle, energy is extracted from the stream due to heat transfer to the walls. This causes a reduction in the stagnation enthalpy of the stream. The energy equation for steady diabatic flow gives the total enthalpy at any point as

$$h_t = h_{t,s}\left(1 - \frac{Q}{wh_{t,s}}\right) \tag{A1}$$

Thus, for no heat transfer the total enthalpy is constant along the nozzle. For real flows, however, total enthalpy continually decreases down the nozzle. The fractional decrease is found from equation (A1) as:

$$\frac{h_{t,s} - h_t}{h_{t,s}} = \frac{Q}{wh_{t,s}} \tag{A2}$$

In this section, an approximate formulation of this decrease is derived to assess the loss in total enthalpy in the inlet.

The total heat transfer in the nozzle inlet is given by

$$Q = \bar{q}A \tag{A3}$$

By analyzing the inlet heating rates, one can verify that up to the throat the heating rate variation is approximately parabolic so that

$$\bar{q} \doteq \frac{1}{3} q^* \tag{A4}$$

to good approximation. Actual measurements confirm this relation (ref. 22). Then, the enthalpy decrement due to heat transfer becomes

$$\frac{h_{t,s} - h_t}{h_{t,s}} \doteq \frac{1}{3} \frac{q^*A}{wh_{t,s}} \tag{A5}$$

The heating rate at the throat section of rocket nozzles has been shown to fit the correlation for flow through heated tubes (ref. 22). Thus, conventional heat-transfer formulas can be used to estimate the forced convection heat-transfer coefficient defined by Newton's cooling law:

$$q^* = H(T_\infty - T_w) = \frac{Hh_t}{\bar{c}_p}\left(1 - \frac{T_w}{T_\infty}\right) \tag{A6}$$

Heat transfer through tubes, for turbulent flow, is given by Nusselt's equation (refs. 23, 24) with quantities evaluated at mean film temperature.

$$Nu = \frac{Hd^*}{k} = 0.026\left(\frac{1 + \frac{T_w}{T_\infty}}{2}\right)^{0.2} Re^{0.8} \tag{A7}$$

For $T_w/T_\infty \approx 1$, which is the case for very low heating rates, this reduces to Nusselt's original correlation. For high heating rates encountered in arc-jet nozzles, this form takes into account the variable transport properties through the boundary layer. For most arc-jet operations, one can take $T_w/T_\infty \approx 1/8$ in the nozzle to simplify the heat-transfer correlation. For this substitution,

$$Nu = 0.023Re^{0.8} \tag{A8}$$

where the Nusselt number and Reynolds number are defined in terms of free-stream properties.

Combining equations (A8), (A6), and (A5) results in a general expression for the enthalpy decrement due to inlet wall heating.

$$\frac{h_{t,s} - h_t}{h_{t,s}} \doteq 0.0082\left(\frac{A}{A^*}\right)\frac{1}{Re^{0.2}} \tag{A9}$$

One finds, for circular-arc inlet geometry the surface to throat area ratio may vary from about 10 to 150 depending on the sharpness of the inlet. For purposes of this consideration, a value of 100 is taken as representative. The Reynolds number in equation (A9) is raised to the 1/5 power; consequently, an order of magnitude estimation is sufficient. For an arc jet operating at 2 megawatts with an efficiency of 50 percent, the Reynolds number can be estimated with the aid of the sonic-flow relation (eq. (12)). For enthalpies between 1,000 and 10,000 Btu/lb and pressures from 10 to 100 atmospheres and taking $d^* = 0.021$ ft as typical, the Reynolds number is found to lie within the limits

$$0.35\times10^5 < Re < 7.8\times10^5$$

A typical value of 10^5 is chosen. Then the enthalpy decrement in the inlet is estimated as

$$\frac{h_{t,s} - h_t}{h_{t,s}} \approx 0.0082 \times 100 \frac{1}{(10^5)^{0.2}} = 0.08$$

For typical operations, then, the enthalpy decrement due to irreversibility in the nozzle inlet is small.

APPENDIX B

DISCHARGE COEFFICIENT FOR A NOZZLE

The discharge coefficient is found by integration of the mass flow rate over the throat area

$$C_D = \frac{\int \rho u \, dA}{w_s} \tag{B1}$$

The variation in density and velocity across the nozzle throat depends on the temperature and velocity profiles. In references 16 and 17, it is shown that the velocity and temperature profiles are essentially identical for a Prandtl number of 1. For air with a Prandtl number of 0.72 and for high heating rates ($T_w/T_\infty \approx 1/8$), the turbulent flow theory given in reference 18 also predicts equality between temperature and velocity fields;

$$\frac{T - T_w}{T_\infty - T_w} = \frac{u}{V_\infty} \tag{B2}$$

This flow-field similarity is adopted here.

The velocity profile through the boundary layer is taken as a power formula of the form

$$\frac{u}{V_\infty} = \left(\frac{y}{\delta}\right)^{1/n} \tag{B3}$$

It can be shown[1] that the Reynolds number of the flow up to the nozzle throat is from 10^5 to 10^6. On the basis of flat-plate experiments, this corresponds to the turbulent flow region. The disturbances produced by an electric-arc discharge in the stagnation chamber will probably induce turbulence at even lower Reynolds numbers.

---

[1]The Reynolds number is defined as $Re = \rho_\infty V_\infty l/\mu_\infty$. The mass velocity is given by the sonic-flow relation (eq. (12)) for enthalpies in the practical range of 1,000 to 10,000 Btu/lb and pressures from 10 to 100 atm as $\rho_\infty V_\infty = 280 p_t/h_t^{0.397} \approx 10 p_t$. The length of boundary-layer run for a circular-arc inlet geometry is $l = d^*(\pi/2)(r_i/d^*) \approx 5d^* \approx 0.1$ ft for $r_i/d^* = 3$ and taking $d^* = 0.021$ ft as typical. In the range considered here

$$0.4\times10^{-4} < \mu_\infty < 10^{-4} \ \frac{\text{lb}}{\text{sec ft}}$$

Then, Reynolds number for the inlet flow is $10^5 < Re < 2\times10^6$.

The integral equation for the nozzle discharge coefficient is obtained by combining equations (B1), (B2), and (B3) where the usual assumption of constant pressure across the boundary layer is employed.

$$C_D = \frac{1}{r^{*2}} \int_0^{r^*-\delta} 2r\, dr + \frac{2}{r^{*2}} \int_{r^*-\delta}^{r^*} \frac{\left(\frac{r^* - r}{\delta}\right)^{1/n} r\, dr}{\frac{z}{z_\infty}\left[\frac{T_w}{T_\infty} + \left(1 - \frac{T_w}{T_\infty}\right)\left(\frac{y}{\delta}\right)^{1/n}\right]} \tag{B4}$$

Making the substitution $r^* - r = y$ and evaluating the first integral gives the required equation

$$C_D = \left(1 - \frac{\delta}{r^*}\right)^2 + 2\left(\frac{\delta}{r^*}\right) \int_0^1 \frac{\left(\frac{y}{\delta}\right)^{1/n} \left[1 - \left(\frac{\delta}{r^*}\right)\left(\frac{y}{\delta}\right)\right] d\left(\frac{y}{\delta}\right)}{\frac{z}{z_\infty}\left[\frac{T_w}{T_\infty} + \left(1 - \frac{T_w}{T_\infty}\right)\left(\frac{y}{\delta}\right)^{1/n}\right]} \tag{B5}$$

In the ranges of enthalpy and pressure considered herein ($10^3 < h_t < 10^4$ Btu/lb and $1 < p_t < 100$ atm), the molecular-weight ratio can be expressed as a function of the temperature and pressure to the required degree of precision of this analysis. One can verify from reference 11 that

where

$$\left.\begin{aligned} z &\approx 1 + cT^3 \\ c &\approx 2.9 \times 10^{-13} p^{-0.22} \end{aligned}\right\} \tag{B6}$$

When (B6) is combined with equations (B2) and (B3), a good approximation to the molecular-weight ratio across the boundary layer is given by:

$$\frac{z}{z_\infty} \approx 1 - \frac{cT_\infty^3}{1 + cT_\infty^3}\left\{1 - \left[\frac{T_w}{T_\infty} + \left(1 - \frac{T_w}{T_\infty}\right)\left(\frac{y}{\delta}\right)^{1/n}\right]^3\right\} \tag{B7}$$

The integral in equation (B5) is not sensitive to the ratio z/z_∞ because it is bounded within rather narrow limits ($2/3 < z/z_\infty < 1$ for the present range considered). Consequently, mean values of $c = 1.8 \times 10^{-13}$ and $T_\infty = 10{,}000^\circ$ R are satisfactory[2] for this study.

[2]Changing the quantity cT_∞^3 by a factor of 8 affects the discharge coefficient given by equation (B5) by less than 5 percent.

REFERENCES

1. Warren, W. R., and Diaconis, N. S.: Air Arc Simulation of Hypersonic Environments. ARS preprint 1986-61.

2. Rose, P., Powers, W., and Hritzay, D.: The Large High Pressure Arc Plasma Generator. AVCO Res. Rep. 56, June 1959.

3. Giannini, Gabriel M.: The Arc Jet. Plasmadyne Corp. M-11, 1959.

4. Eschenback, R. C., and Skinner, G. M.: Study of Arc Heaters for a Hypersonic Wind Tunnel. WADD TR 60-354, May 1960.

5. Cason, C. M., Barr, T. A., and Roberts, T. G.: The ARGMA Plasma-Jet Facility. A Résumé, 1958-1960. TN 2H2N, Army Rocket and Guided Missile Agency, 1961.

6. Gowen, F. E., and Hopkins, V. D.: A Wind Tunnel Using Arc-Heated Air for Mach Numbers From 10 to 20. Second National Symposium on Hypervelocity Techniques, Denver, Colorado, March 1962, pp. 27-46.

7. Nagler, Robert G.: Application of Spectroscopic Temperature Measuring Methods to Definition of a Plasma Arc Flame. Jet Propulsion Lab. Tech. Rep. 32-66, 1961.

8. Warren, W. R.: Determination of Air Stagnation Properties in a High Enthalpy Test Facility. JAS/SS, vol. 26, no. 12, 1959.

9. Liepmann, Hans W., and Puckett, A. E.: Introduction to Aerodynamics of a Compressible Fluid. John Wiley and Sons, N. Y., 1947.

10. Cobine, James D.: Gaseous Conductors. Dover Pub., N. Y., 1941.

11. Moeckel, Wolfgang, and Weston, K. C.: Composition and Thermodynamic Properties of Air in Chemical Equilibrium. NACA TN 4265, 1958.

12. Yoshikawa, Kenneth K., and Katzen, E. D.: Charts for Air-Flow Properties in Equilibrium and Frozen Flows in Hypervelocity Nozzles. NASA TN D-693, 1961.

13. Compton, Dale L., Winovich, W., and Wakefield, R. N.: Measurements of the Effective Heats of Ablation of Teflon and Polyethylene at Convective Heating Rates From 25 to 420 Btu/ft^2/sec. NASA TN D-1332, 1962.

14. Camac, M., and Vaughn, A.: Oxygen Vibration and Dissociation Rates in Oxygen-Argon Mixtures. AVCO Res. Rep. 84, Dec. 1959.

15. Wilson, J.: A Measurement of the Recombination Rate of Oxygen. Cornell Univ., Ithaca, N. Y., ONR Contract NONR 401 (25). Graduate School of Aeronautical Engr., June 1962.

16. Boelter, L. M. K., Martinelli, R. C., and Jonassen, F.: Remarks on the Analogy Between Heat Transfer and Momentum Transfer. Trans. ASME, vol. 63, July 1941, pp. 447-55.

17. Shapiro, A. H.: The Dynamics and Thermodynamics of Compressible Fluid Flow. Vol. II. The Ronald Press Co., N. Y., 1954.

18. Schlichting, H.: Boundary Layer Theory. McGraw-Hill Book Co., N. Y., 1955.

19. Mager, Artur: Approximate Solution of Isentropic Swirling Flow Through a Nozzle. ARS, vol. 31, no. 8, 1961, pp. 1140-1148.

20. Fay, J. A., and Riddell, F. R.: Theory of Stagnation Point Heat Transfer in Dissociated Air. Jour. Aero. Sci., vol. 25, no. 2, 1958, pp. 73-85.

21. Hoshizaki, H.: Mass Transfer and Shock Generated Vorticity. ARS Journal, vol. 30, no. 7, 1960, pp. 628-634.

22. Greenfield, Stanley: Determination of Rocket-Motor Heat-Transfer Coefficients by the Transient Method. Jour. Aero. Sci., vol. 18, no. 8, 1951, pp. 512-518.

23. McAdams, W. H.: Heat Transmission. McGraw-Hill Book Co., N. Y., 1942.

24. Eckert, E. R. G.: Introduction to the Transfer of Heat and Mass. McGraw-Hill Book Co., N. Y., 1950.

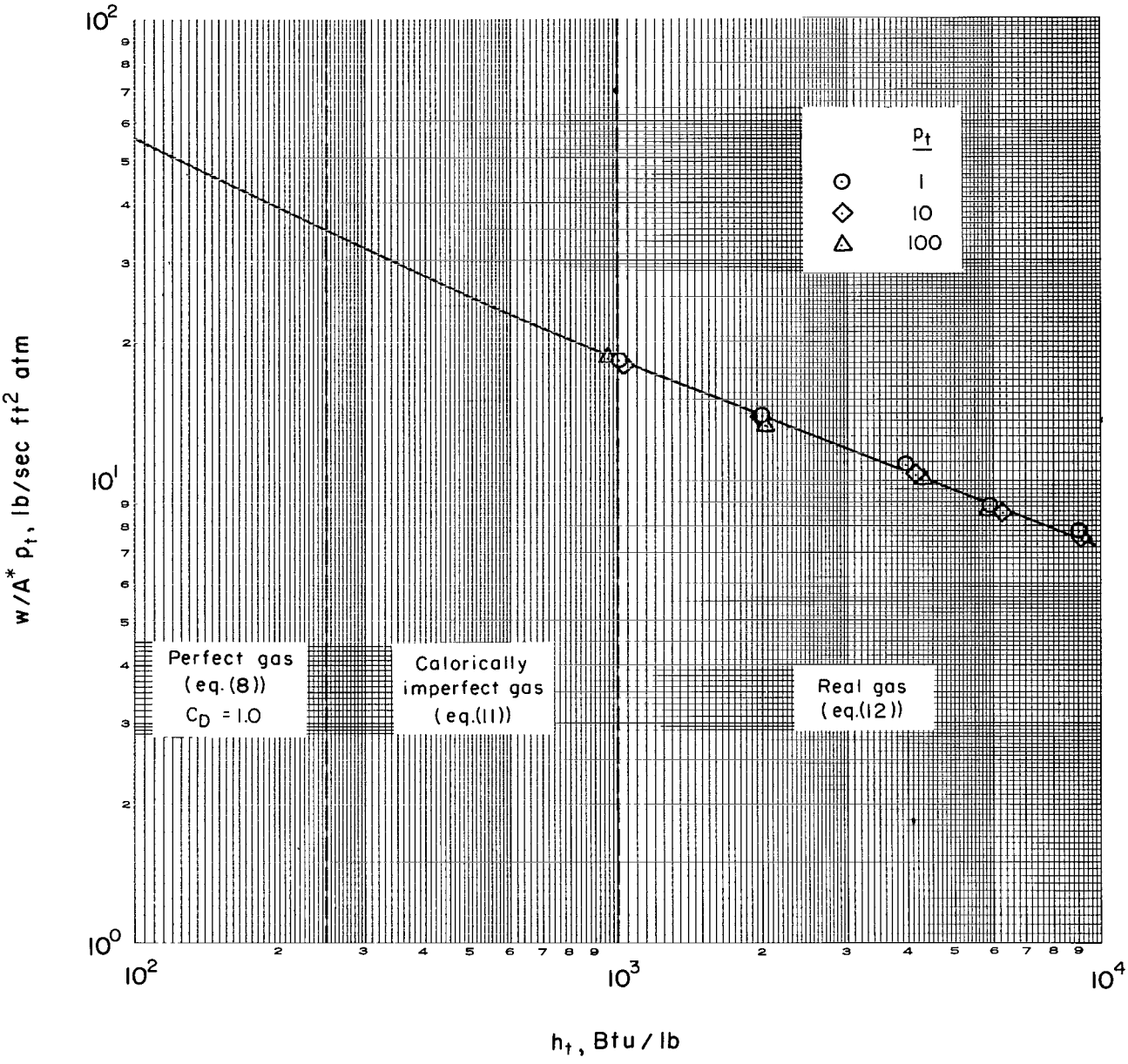

Figure 1.- Equilibrium sonic-flow formulation for air.

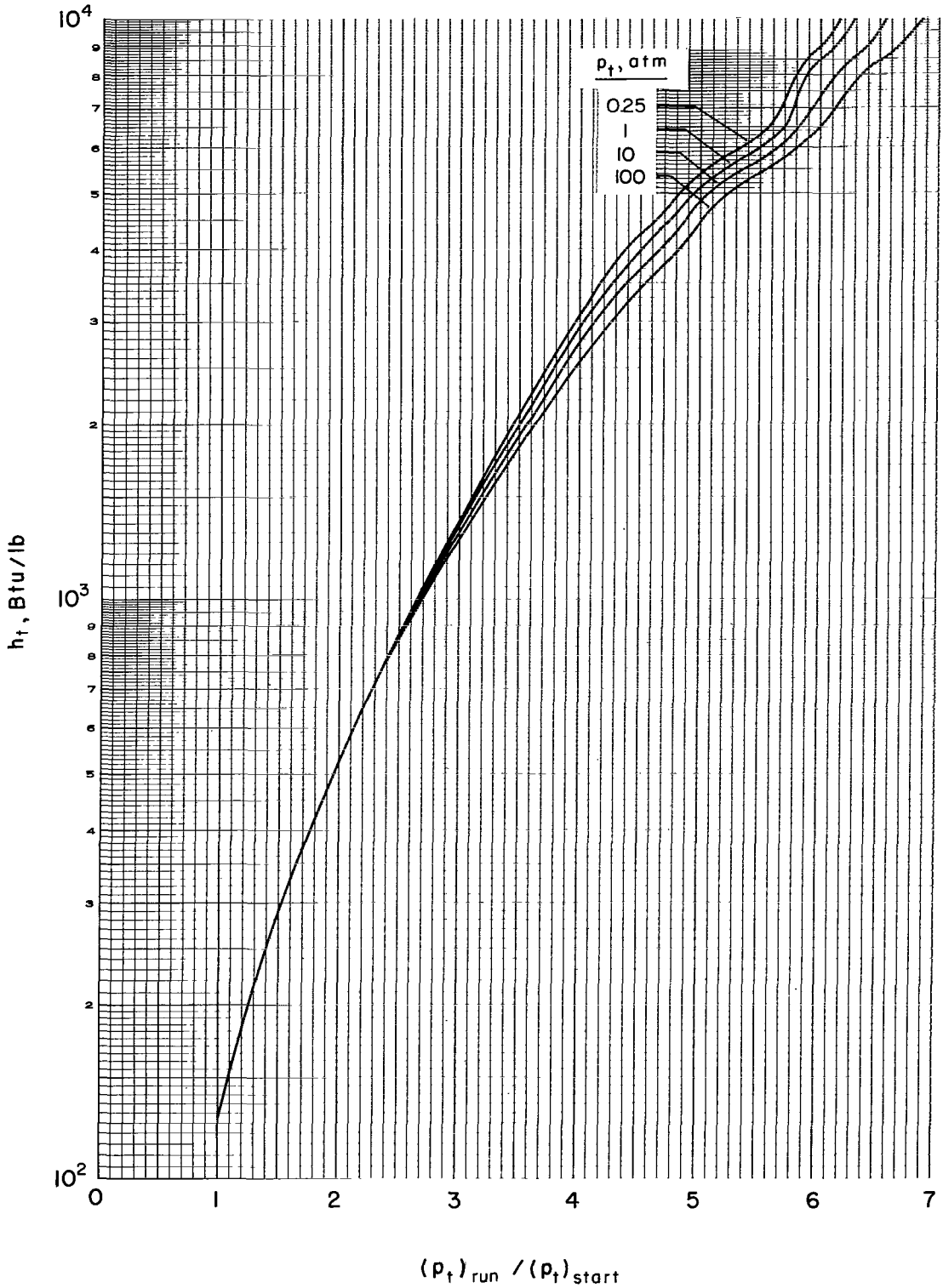

Figure 2.- Pressure-rise technique for enthalpy determination; ambient starting conditions.

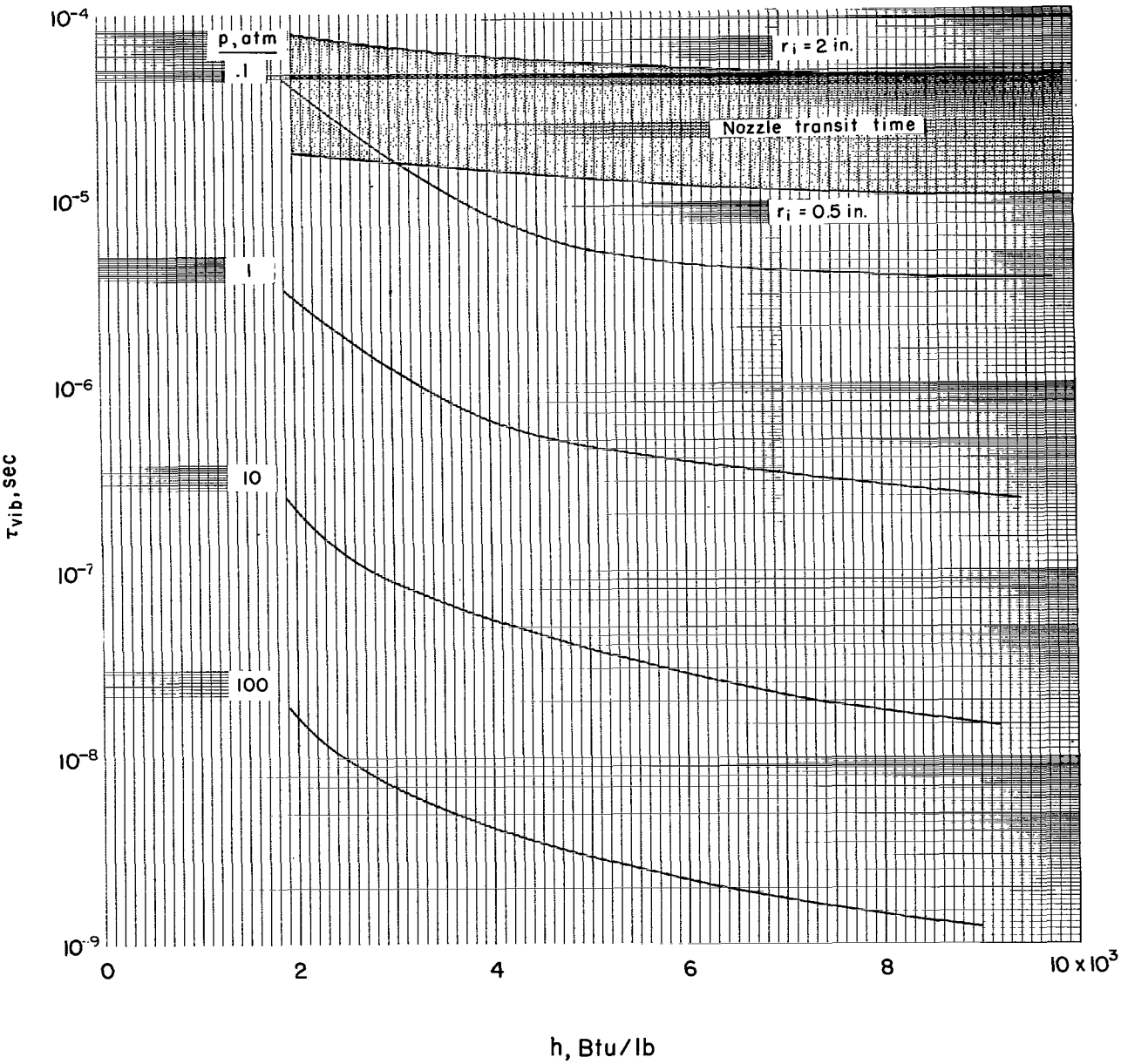

Figure 3.- Vibrational relaxation time for air in the high-pressure arc range.

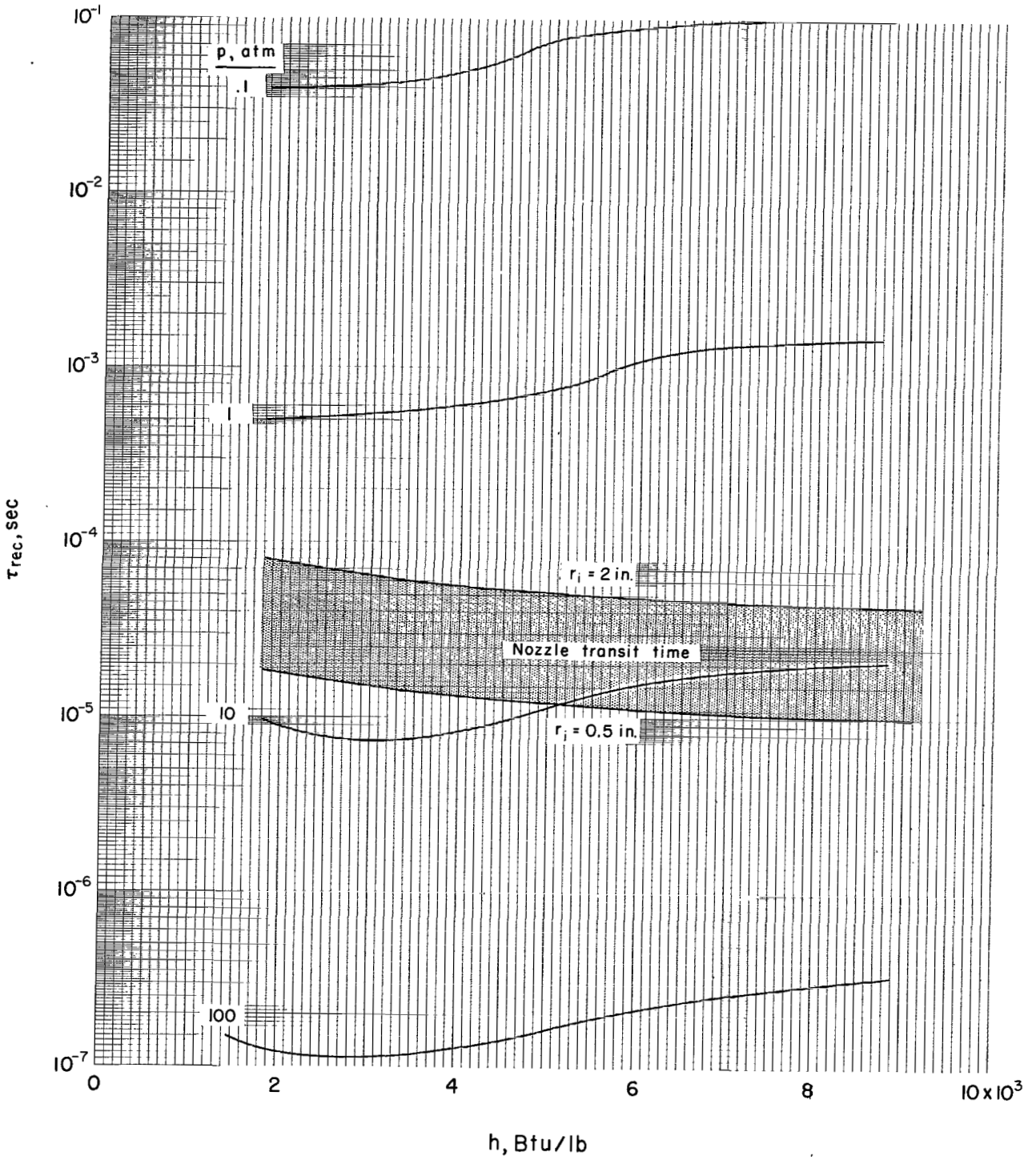

Figure 4.- Chemical recombination time for oxygen in the high-pressure arc range.

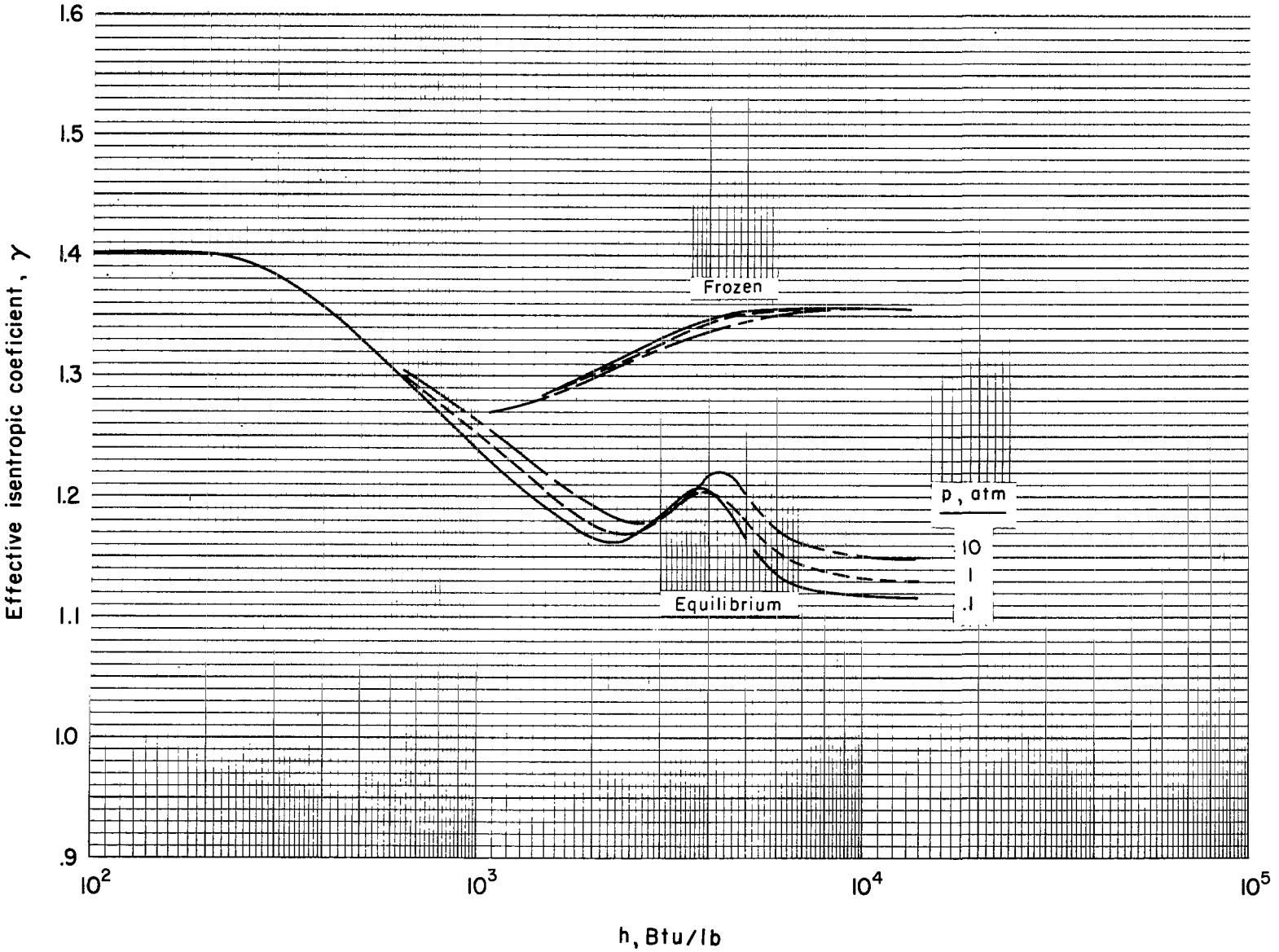

Figure 5.- Effective isentropic coefficient for chemically frozen and equilibrium nozzle flows for air.

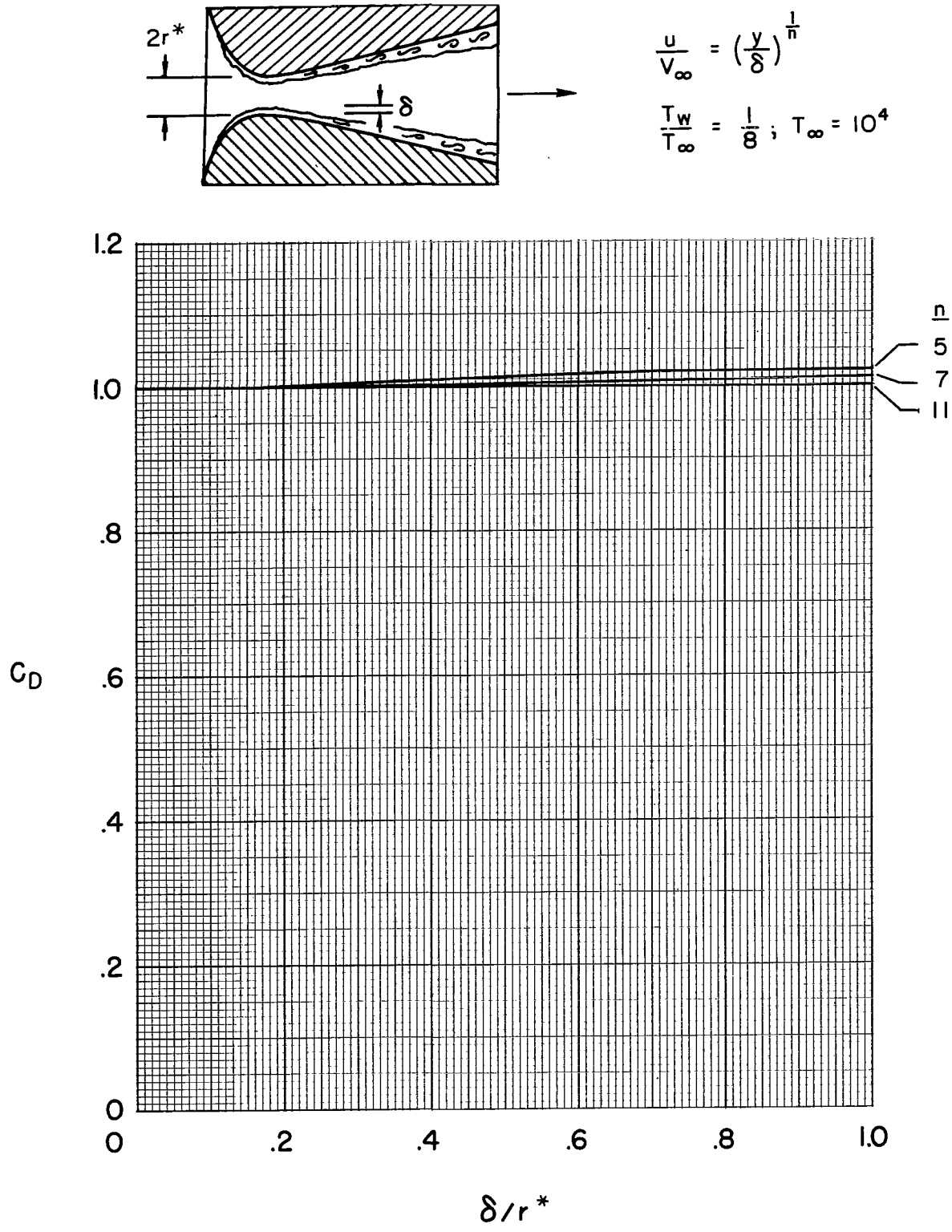

Figure 6.- Effect of velocity profile and boundary-layer thickness on discharge coefficient for high heating rates.

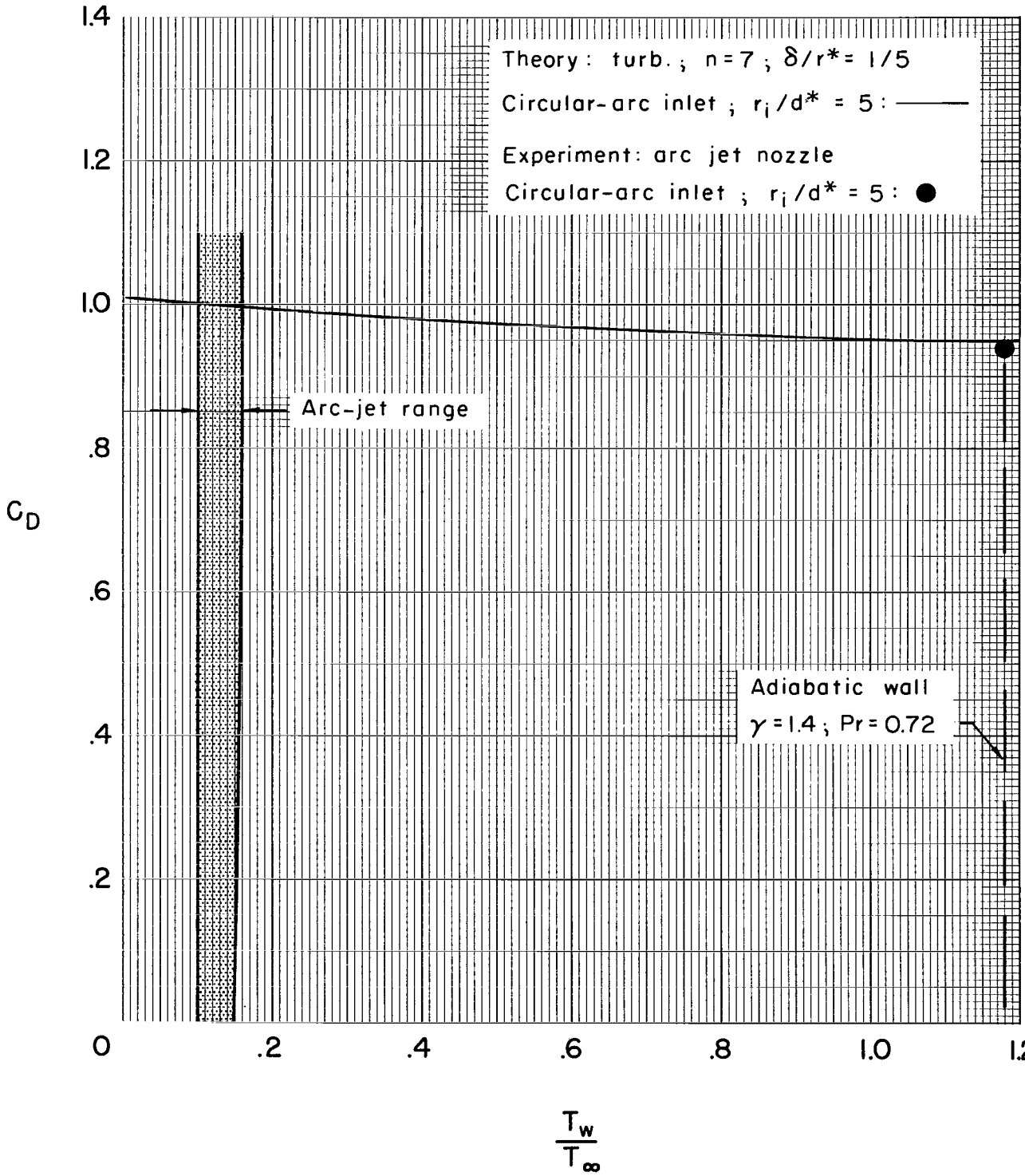

Figure 7.- Variation of arc-jet nozzle discharge coefficient with wall-temperature ratio.

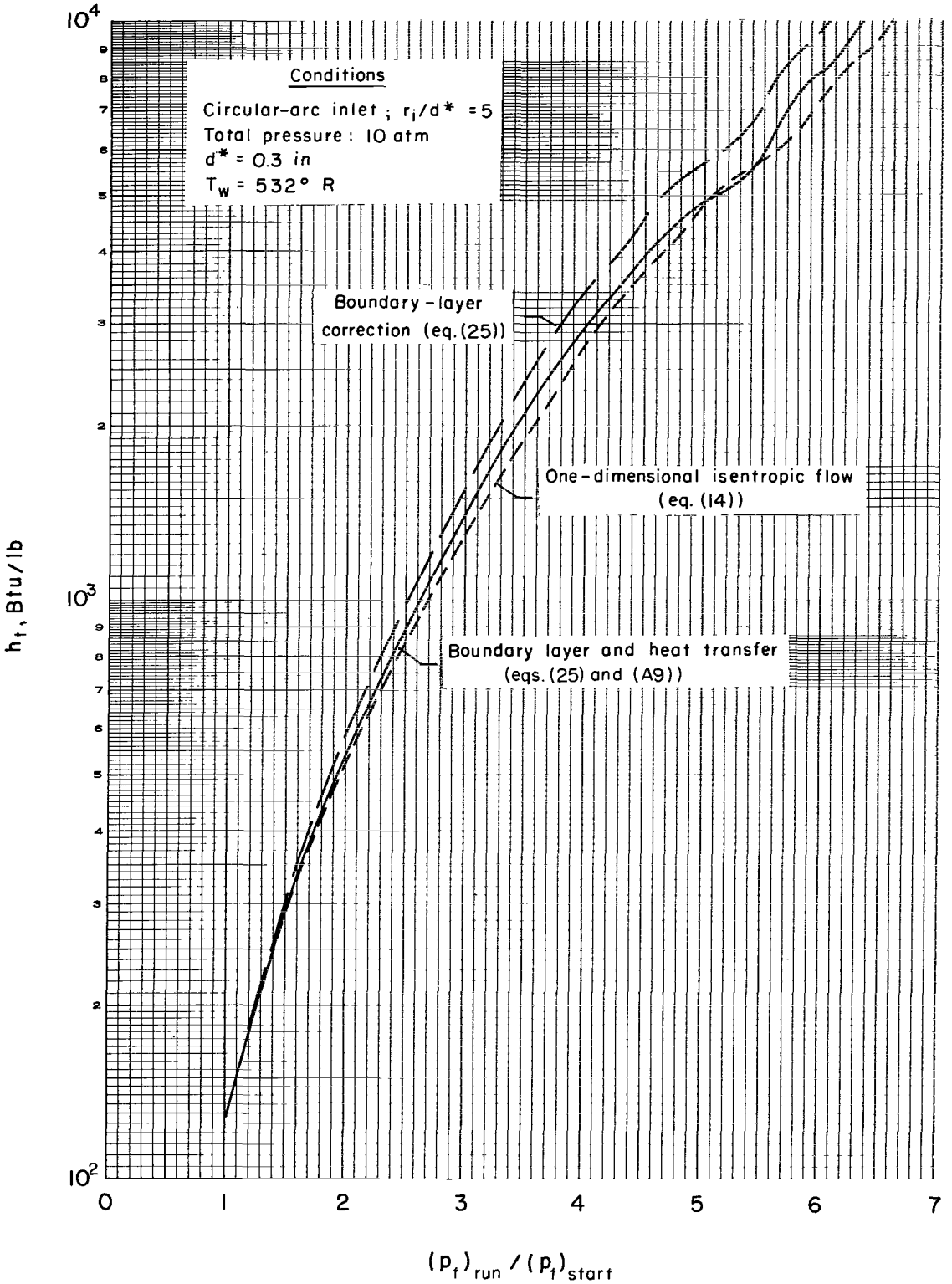

Figure 8.- Effect of nozzle boundary layer and nozzle inlet heating on enthalpy determined by pressure-rise technique.

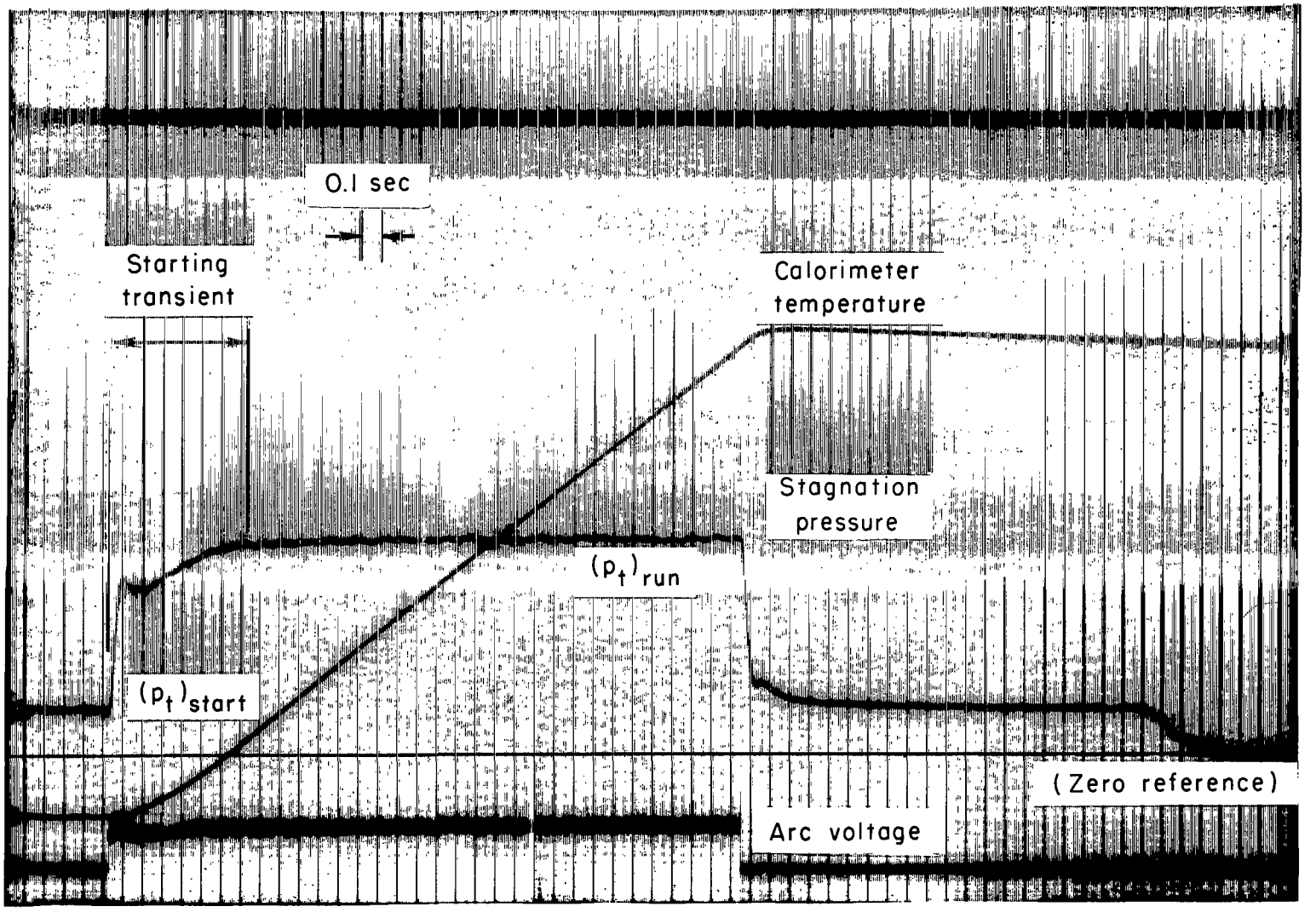

Figure 9.- Typical run record illustrating pressure-rise technique for enthalpy measurement; $(p_t)_{run}/(p_t)_{start} = 4.60$; $p_t = 0.25$ atmosphere; $h_t = 4{,}500$ Btu/lb from figure 2.

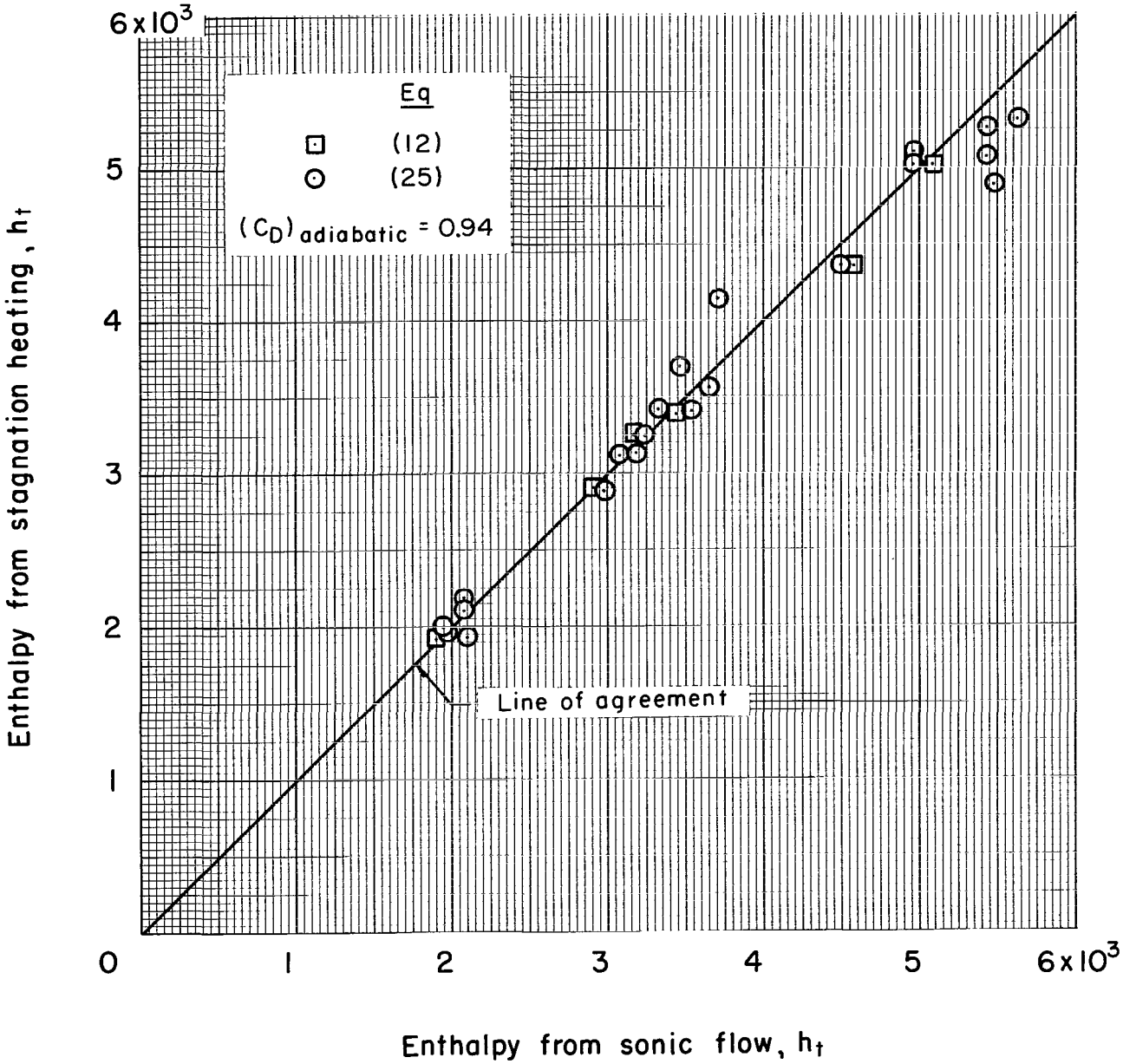

Figure 10.- Comparison of enthalpy deduced from stagnation-point heating with sonic-flow enthalpy deduced from measured flow rate (eq. (12)) and from pressure-rise technique (eq. (25)).